



Role of influence-induced dynamic link weight adjustment in the cooperation of spatial prisoner's dilemma game

Chengli Zhao^{1,a} and Xue Zhang¹

¹ College of Liberal Arts and Sciences, National University of Defense Technology, Changsha, 410073, China

Received 20 January 2021 / Accepted 6 March 2021 / Published online 27 May 2021

© The Author(s), under exclusive licence to EDP Sciences, SIF and Springer-Verlag GmbH Germany, part of Springer Nature 2021

Abstract. We propose a novel dynamic link weight adjustment model, in which link weights on static network will be dynamically adjusted according to agents' influence during the evolutionary process. To be specific, when an agent's strategy is learned by one of his direct neighbors, his influence will be expanded by one unit β . Then link weights between agents will be adaptively adjusted by counting the influence of agents. Meanwhile, we utilize a variable δ to control the range of link weights, that is, link weights can only be limited within the interval $[1 - \delta, 1 + \delta]$. In our model, it should be noted that link weights between agents will be integrated into the fitness calculation process. Through abundant simulations, the results indicate that the newly proposed model can significantly foster the persistence and emergence of cooperation. In addition, when the cost-to-benefit ratio u is quite small, the level of cooperation will increase with the augmentation of δ . However, when the cost-to-benefit ratio u exceeds a certain value, the level of cooperation increases at the early stage and then decreases with the growth of δ . As for the potential reasons, we observe that it is closely related to the type of connections, in which the cooperation can flourish once $C - C$ type links dominate the system, while other types will hamper the evolution of cooperation. Taking together, the current model and results will provide some insights into the collective cooperation within the human population.

1 Introduction

It is well known that the cooperation between selfish individuals greatly benefits the development of human society [1]. However, the donation of cooperators within the population will benefit their opponents, especially defectors, at the cost of their own losses, which will give rise to the conflict between altruism and egoistic behavior [2], and thus even induce the so-called social dilemmas [3]. Therefore, deeply understanding the ubiquitous cooperation among irrelevant and selfish agents has puzzled for a long time [4–7]. Furthermore, to explain the potential reasons for the emergence of cooperation or explore the incentive mechanisms for the maintenance of cooperation, scholars in various fields have tried their best to solve this issue from both theoretical and empirical efforts [8–13].

Fortunately, evolutionary game theory (EGT) [14–16] provides a simple yet powerful framework to investigate the problem of the evolutionary cooperation. In particular, over the past decades, prisoner's dilemma game (PDG) [17–22], as the famous pairwise interaction game model, has been generally used to illustrate the

conflict between individual interest and social welfare. In the traditional PDG, two agents must simultaneously make a decision to cooperate (C) or defect (D) without knowing the opponent's strategy during the game process. In addition, when two cooperators encounter, they will gain the reward R for their mutual cooperation; while two defectors come across, they will get the punishment P for their defection. However, if a cooperator meets with a defector, the former will be exploited and have to receive the worse payoff S , but the latter reaps the benefit to get the maximum payoff T during the pairwise interaction. Furthermore, all these parameters need to fulfill the ranking order $T > R > P > S$ and the condition $2R > T + S$. There is no doubt that all agents in a well-mixed population, due to their inherent selfishness, will inevitably be defected in the end, even if the mutual cooperation leads to the stable gains for each other and is beneficial to the whole population.

Meanwhile, with the rapid development of network science, more and more researchers have found that agents can only interact with a limited number of direct neighbors. Particularly, Nowak and May semi-investigated the evolutionary dynamics of PDG on the spatially regular lattice with the fixed neighborhood, revealing that the cooperative agents on spatial structures can be organized into the tight clusters to

^a e-mail: chenglizhao@nudt.edu.cn (corresponding author)

resist the attack and exploitation from defectors, which is known as the spatial or network reciprocity [23]. After that, numerous different underlying topologies have also been successfully confirmed to contribute to the evolutionary cooperation, which include small-world [24], scale-free [25] and independent or multi-layer networks [26, 27], to name but a few. Moreover, to explore how to facilitate the evolution of cooperation, some additional incentive mechanism have also been proposed, for instance, reputation [28, 29], mobility [30, 31], information sharing [32, 33], memory effect [34, 35], multigames [36, 37] and so on, to further facilitate the persistence and emergence of collective cooperation.

Although some previous works have significantly contributed to the evolution of cooperation, the impact of dynamic adjustment of link weight between agents on evolutionary cooperation also cannot be ignored. For instance, inspired by the time-varying and heterogeneous phenomena of inter-individual dependence, Huang et al. proposed a coevolutionary game model of strategy and link weight, which indicated that the frequency of cooperation could be maintained at a higher level even in the case of larger temptation to defect [38]. Shen et al. presented an aspiration-based coevolutionary game model of dynamic link weight adjustment, and investigated the impact of this dynamic adjustment mechanism on the evolution of cooperation in the spatial PDG [39]. From the perspective of time-scale heterogeneity, Chu et al. found that the coevolutionary strategy and link weight could significantly promote cooperation in spatial structures [40]. Guo et al. believed that interaction could cause the heterogeneity of reputation, which further induced the heterogeneity of link weights. Thus, they gave a reputation-based coevolutionary link weights model [41]. Actually, some intrinsic attributes of agents will constantly change with the interaction, which inevitably gives rise to the dynamic adjustment of link weights between agents. However, there is still an important factor being overlooked, that is, the influence of agents during the game process. In our life, if an agent's idea or strategy is learned or adopted by his neighbors, then his influence will be expanded, and contracted otherwise. Meanwhile, the heterogeneity of influence among agents necessarily induces the dynamic adjustment of link weights. To this end, in this work, we make an end to explore how the influence-induced dynamic adjustment of link weights between agents will affect the evolution of cooperation.

The remaining sections of the paper will be arranged as follows. First, the model will be defined in detail in Sect. 2. Then large quantities of simulations will be presented and discussed in depth in Sect. 3. Finally, we will provide some concluding remarks in Sect. 4.

2 Mathematical model

In this paper, agents play a coevolutionary game with their direct neighbors on fully populated lattice, in

which the lattice size is set to be $L \times L$ and fulfil the periodic boundary condition. In addition, each player will play the game with his 4 direct neighbors, that is, Von Neumann neighborhood is assumed here. Meanwhile, we mainly take an evolutionary PDG to depict the potential social dilemmas. During the evolutionary PDG process, two agents must simultaneously decide either to cooperate or to defect without knowing the strategy or action of their opponents in advance. Following the common practice [42–44], in the donation game version of PDG, a cooperator must bear a cost of c to make his opponent to gain the benefit of b . Thus, the payoff values of PDG are set to be $T = b$, $S = -c$, $R = b - c$ and $P = 0$. For any $b > c$, we can find that the strict payoff ranking $T > R > P > S$ can be followed. Generally, the payoff matrix of the current PDG model can be further re-scaled as

$$M = \begin{pmatrix} 1 & -u \\ 1 + u & 0 \end{pmatrix}, \quad (1)$$

where $u = c/(b - c)$ means the so-called cost-to-benefit ratio. It should be noted that simulations of the model are carried out through Monte Carlo steps (MCS), and the inner steps of each MCS consist of the following substeps.

Initially, each player x can be stochastically and equally chosen as a cooperating agent [$C, s_x = (1, 0)^T$] or a defecting one [$D, s_x = (0, 1)^T$], that is, x can become a cooperator or defector at the first MCS step with the probability 50%. In the meantime, each agent has an additional influence attribute I_x with an initial value of 1, which can be dynamically adjusted according to strategy imitation. Furthermore, every link weight between agents has the same initial value $w = 1$, which will also be dynamically adjusted according to their dynamic influence. For each time step during the game interaction, any agent x can be chosen as the focal player once on average. Then player x will calculate his initial payoff through playing the game with one of his direct neighbors as follows:

$$p_{xy} = s_x^T M s_y. \quad (2)$$

After that, the focal agent x will accumulate his fitness F_x by combining the initial payoff p_{xy} with the corresponding link weight w_{xy} between player x and his direct neighbor y , which sums over all 4 nearest neighbors as follows:

$$F_x = \sum_{y \in \Omega_x} w_{xy} * p_{xy}, \quad (3)$$

where Ω_x denotes the set of all nearest neighbors of player x and $|\Omega_x| = 4$.

Next, the system enters the phase of strategy updating. To be specific, the focal agent x will pick up one direct neighbor y at random, in which player y will also acquire his accumulated fitness F_y in the same

way of the focal agent x . After that, agent x can asynchronously update his strategy through comparing his current accumulated fitness F_x with the accumulated fitness F_y of y according to the Fermi rule [45],

$$W = \frac{1}{1 + \exp[(F_x - F_y)/K]}, \tag{4}$$

where the parameter K is the noise factor, which can capture irrational errors in the process of strategy imitation. Although the focal agent x can learn the strategy of his direct neighbor y if $F_x < F_y$, it may be also possible that the focal agent x drops y 's strategy when $F_x > F_y$. Considering that the effect of parameter K has been well explored in the previous works [46, 47], we will set $K = 0.1$ in this work without lacking the generality. If the focal agent x succeeds in adopting the strategy of his direct neighbor y , it means that the neighbor y 's influence will be magnified by the value of β [48], which can be expressed quantitatively by the following formula:

$$I_y = I_y + \beta, \tag{5}$$

where the parameter β is the increment of agent y 's influence. Within this work, we will prove that if the parameter β is positive, no matter what the value of β is, the evolutionary results will not change significantly. After the influence of one individual agent is varied, the link weight between this agent and his opponent will be changed accordingly. As an example, the link weight between two interacting partners x and y can be adjusted according to the influence relationship as follows [29, 38, 41, 49]:

$$w_{xy} = \begin{cases} w_{xy} + \Delta & \text{if } I_x < I_y, \\ w_{xy} - \Delta & \text{if } I_x > I_y, \\ w_{xy} & \text{otherwise,} \end{cases} \tag{6}$$

where the parameter $\Delta \in [0, 1)$ is the manipulating variable of the link weight. In line with previous works [29, 38, 41], the link weight is often assumed to be varied within the interval $[1 - \delta, 1 + \delta]$, in which $\delta \in [0, 1)$ determines the potentially limiting values of link weights. Obviously, when $\Delta = 0$ or $\delta = 0$, the link weights are frozen (i.e. all link weights keep the initial value $w = 1$), which means that the system degrades into the traditional static network situation, that is, only strategies can evolve.

Once the aforementioned sub-steps are completed, one full Monte Carlo Simulation (MCS) step will be ended, within which all agents have one chance to update their strategy on average. The current results are mainly carried out on 100×100 square lattice. To eliminate the finite-size effect, the larger lattice size (such as $L = 200$ or 400) is also tested and the identical simulation results are obtained although they are not presented here. Moreover, the key quantity ρ_C (the frequency of cooperation) to measure the model performance is determined by averaging over the last 2×10^3 MCS steps for the whole 3×10^4 steps, which ensures the system to arrive at a stable state. Furthermore, to avoid

the interference of random factors, the final results are averaged over at least 20 independent simulations for each set of parameters.

3 Results and analyses

To verify the validity the model to promote and maintain the evolution of cooperation, we first inspect how the frequency of cooperation ρ_c varies with the cost-to-benefit ratio u for several values of δ in Fig. 1. According to the potential interaction network structure, rule of strategy updating and other details of simulation, there is always a critical threshold u_c beyond which defectors will dominate the whole system. Thus, we are not only interested in how much the frequency of cooperation ρ_c has increased under the proposed mechanism, but also concerned with how the new mechanism can effectively enlarge the critical value u_c . When $\delta = 0.0$, all link weights are frozen at the initial value of 1, which means that the system degenerates into its traditional form. Thus, the frequency of cooperation ρ_c is quickly down to zero with the increase of u , and the critical threshold u_c is at about 0.0215, which is in line with the previous work [43]. However, once $\delta > 0$, the evolution of cooperation is significantly improved even if the level of cooperation still continues to decline as u increases. In comparison with the traditional case, not only the frequency of cooperation ρ_c has been greatly enhanced, but also the critical value of cooperators dying out u_c has also been markedly enlarged. Even when δ increases up to

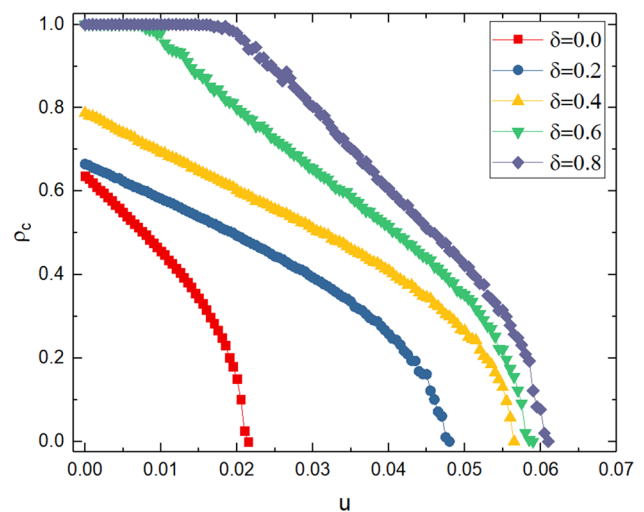


Fig. 1 Frequency of cooperation ρ_c as a function of cost-to-benefit ratio u for several different values of δ . When $\delta = 0$, the system degenerates into the traditional situation. However, when $\delta > 0$, link weights in the system is no longer maintained at the value of 1, but dynamically adjusted as the system evolves. It can be found that the level of cooperation can be gradually elevated with the increase of u . All simulation results are obtained for the parameter setup: $L = 100$, $MCS = 3 \times 10^4$, $\Delta = 0.1$, $K = 0.1$, and $\beta = 1$

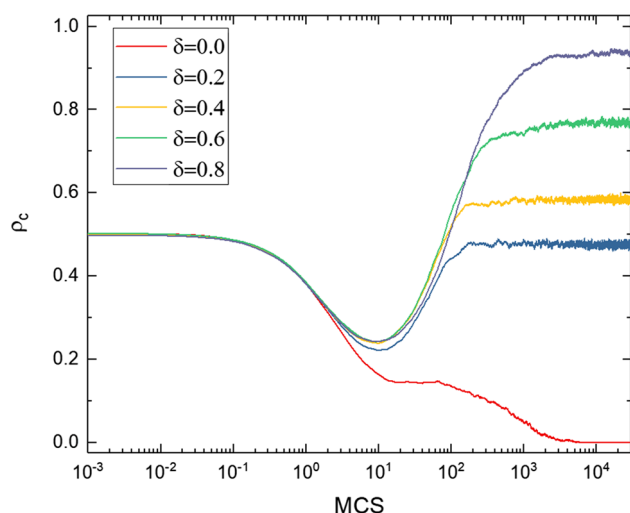


Fig. 2 Time courses of frequency of cooperation ρ_c for several different values of δ when the cost-to-benefit ratio $u = 0.022$. It can be found that cooperators continues to decline until dies out when $\delta = 0.0$. However, when $\delta > 0$, the frequency of cooperation ρ_c experiences a process of decrease at first and then increase over time. In addition, the larger value of δ will lead to the higher frequency of cooperation within the population. Other parameters are set as Fig. 1

a certain threshold, there is a situation (for instance $\delta = 0.6$ or $\delta = 0.8$), in which cooperators can occupy the whole system. All of these macroscopic results indicate that the proposed mechanism is effective in facilitating the evolution of cooperation.

Then we need to further explore the role of the proposed mechanism in the microscopic evolution of collective cooperation, which will help us to capture more details during the process of evolution. To this end, Fig. 2 provides time courses of the frequency of cooperation ρ_c for several values of δ when the cost-to-benefit ratio is fixed to be $u = 0.022$. Following the previous works [50,51], a complete evolutionary process can be divided into two sub-sequential stages, that is, the enduring (END) phase and expanding (EXP) phase. To be specific, in the initial stage cooperators are subject to attacks and invaded by defectors since there are strong social dilemmas in the system and defectors occupy favorable terrain. Therefore, the level of cooperation continues to decline during this stage, which is called the END phase. Then, with the help of network reciprocity and the proposed mechanism, cooperators try their best to switch from the defense into the offense. Henceforth, the level of cooperation begins to rise gradually, which is defined as the EXP phase. For $\delta = 0.0$, all link weights are left at the initial value of 1, which corresponds to the traditional situation. At this point, cooperators can only rely on network reciprocity to counter the defectors' exploitation. It is clear that cooperators continues to nonlinearly decline over time until they completely disappears regardless of their attempts to defy the defectors but ultimately to no avail, that is,

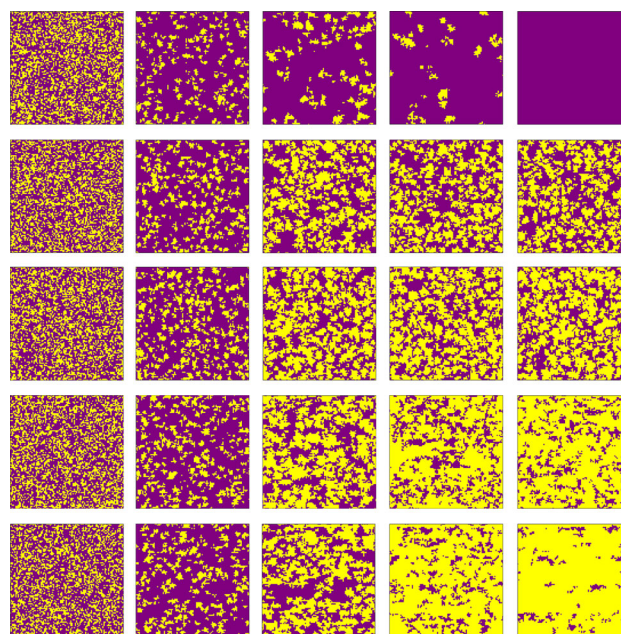


Fig. 3 Snapshots of spatial strategy evolution in some particular state. From top to bottom, each line of results are obtained at $\delta = 0.0$, $\delta = 0.2$, $\delta = 0.4$, $\delta = 0.6$, and $\delta = 0.8$, respectively. Meanwhile, from left to right, each column of snapshots are taken at $MCS = 0, 10, 100, 500, \text{ and } 30,000$, respectively. Moreover, yellow dots and purple spots stand for cooperative and defective strategies, respectively. Other parameters are set as those in Fig. 1

there is only END stage at $\delta = 0.0$ while the EXP one is absent. However, once the proposed mechanism is introduced into the system, network reciprocity can be greatly enhanced. For $\delta > 0$, not only can the downward momentum of the level of cooperation be held at the final END phase, but also the level of cooperation can progressively go up to a different altitude for various value of δ during the EXP phase. Moreover, the larger value of δ will lead to the higher frequency of cooperation within the population. As an example, during the equilibrium phase, when $\delta = 0.2$, the frequency of cooperation ρ_c can be restored to a level slightly below the initial value, while for $\delta = 0.8$, ρ_c can climb to around 0.9, which indicates that the proposed mechanism is effective in promoting the evolution of cooperation.

In addition, to visually comprehend the impact of the proposed influence-induced dynamically adjusted link weight mechanism on the evolution of cooperation, we scrutinize the evolutionary state of the strategy through some representative snapshots in Fig. 3. In Fig. 3, all snapshots are obtained at $u = 0.022$. Meanwhile, yellow dots and purple ones stand for cooperators and defectors, respectively. For each row from top to bottom, the parameter δ is fixed as 0.0, 0.2, 0.4, 0.6 and 0.8, respectively. For each column from left to right, the MCS are set to be 0, 10, 100, 500 and 30000, respectively. Initially, cooperators and defectors are evenly distributed within the population with the equal probability. Thus, it can be found that there is no significant difference

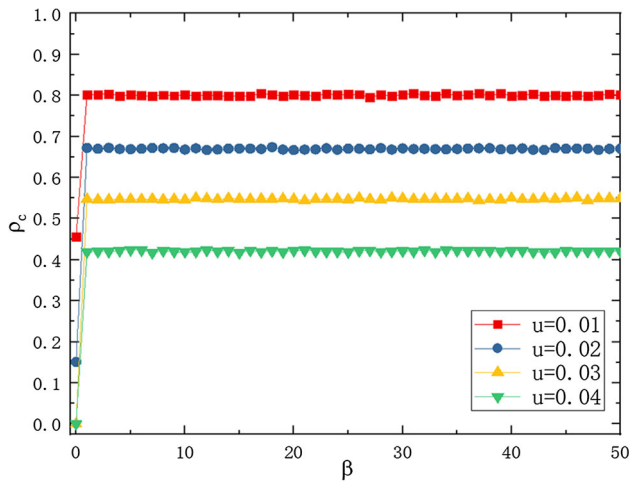


Fig. 4 Frequency of cooperation ρ_c in dependence on the increment of agents' influence β for several different values of cost-to-benefit ratio u . It can be found that once the parameter β is greater than 0, the ρ_c does not seem to change no matter how much β increases, which indicates that β is not the direct factor affecting the evolution of cooperation. The simulation results are obtained at $MCS = 3 \times 10^4$, $L = 100$, $\Delta = 0.1$, $\delta = 0.5$ and $K = 0.1$

for the snapshots taken under any parameter δ when $MCS = 0$. However, once the system begins to evolve, there are obvious differences in snapshots under different values of δ . For instance, when $\delta = 0.0$, cooperators have to gang up against the defector's attack with the help of network reciprocity. It can be found that there are some quite tight yellow star clusters in the purple ocean when $MCS = 10$. Over time, the tight yellow star clusters become larger but fewer when $MCS = 100$ and 500. One can find that cooperators are struggling to get rid of the exploitation by the defectors. However, due to strong social dilemmas, it seems futile as they ultimately tend to be extinct. In stark contrast, after the proposed mechanism is introduced into the system, one can find that cooperation has become more and more prosperous with the increase of δ even if the level of cooperation also declines at $MCS = 10$. Moreover, the larger the value of δ , the wider the yellow area in the stable state. Taking $\delta = 0.8$ as an example, yellow cooperators nearly occupy the entire system while purple defectors are scattered across the yellow sea. All these observations indicate that network reciprocity can be enhanced by the proposed mechanism, which can further confirm that the current mechanism favors the evolution of cooperation.

It should be emphasized that all the aforementioned results are obtained at the increment of agents' influence of $\beta = 1$. To further investigate the impact of parameter β on the frequency of cooperation ρ_c , Fig. 4 plots ρ_c in dependence on the increment of agents' influence of β for several different values of cost-to-benefit ratio u . When $\beta = 0$, it signifies that agents' influence cannot be changed even if their strategies are learned so that link weights between agents also cannot be dynam-

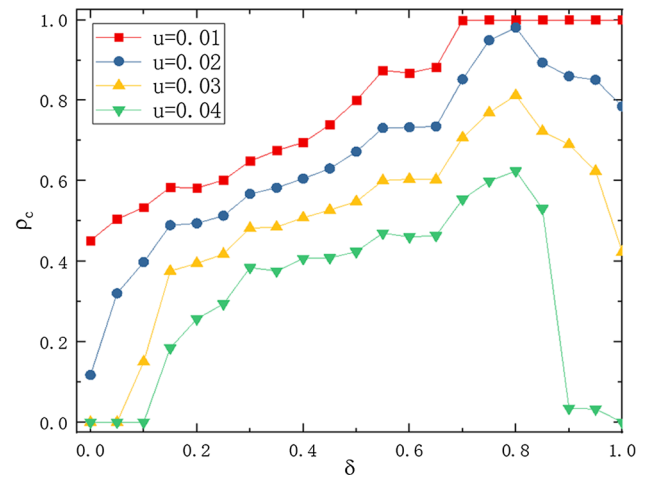


Fig. 5 Frequency of cooperation ρ_c as a function of δ at several different given values of cost-to-benefit ratio u . When the cost-to-benefit ratio u is quite small, ρ_c continues to increase with the increase of δ . However, when the cost-to-benefit ratio u exceeds a certain value, ρ_c goes through first increase and then decrease, which means that there is an optimal value of δ ($\delta = 0.8$) facilitating the evolution of cooperation. The simulation results are obtained at $MCS = 3 \times 10^4$, $L = 100$, $\Delta = 0.1$, $\beta = 1$ and $K = 0.1$

ically adjusted, which leads to the system equivalent to the traditional case. However, when $\beta \neq 0$, agents' influence will be changed if their strategies are adopted. Thus, the uneven influence of the agents inevitably leads to the heterogeneous link weights, which makes the level of cooperation greatly improved. Surprisingly, the frequency of cooperation ρ_c will not be significantly changed with the increase of β , which indicates that the parameter β is not the direct factor affecting the evolution of cooperation. In fact, in our model, the parameter β just cause the uneven or heterogeneous influence between agents, and thus it plays an indirect role in maintaining the high level of cooperation. Meanwhile, it will be demonstrated later that the heterogeneous link weights induced by agents' asymmetrical influence play a significant role in determining the evolution of cooperation. Thus, without loss of generality, we always assume the parameter $\beta = 1$ in the following results.

Next, since we just analyze the impact of the parameter δ with limited values on the cooperation in the previous figures, it will be worthwhile to widely explore how δ affects the evolutionary dynamics of the cooperation. To this end, for several other values of u , we depict the frequency of cooperation ρ_c as a function of δ in Fig. 5. From Fig. 5, it can be found that the parameter δ plays a significant role in facilitating the collective cooperation within the population. However, for different values of u , there are also some slightly differences for parameter δ to influence the level of cooperation. For instance, when u is quite small (e.g. $u = 0.01$), ρ_c increases monotonously as δ increases until the full cooperation is reached. Nevertheless, when u increases up to a certain value, ρ_c no longer increases monotonously with

the increase of δ . On the contrary, with the increase of δ , ρ_c shows a single hump trend, that is, the bell-shape curves are exhibited. What is more, the peaks all occurs around $\delta = 0.8$, and a smaller or larger δ will lead to a decreasing trend as far as the level of cooperation is concerned. It can be clearly found that when δ increases from zero, the frequency of cooperation ρ_c first goes through the increase until the maximum frequency of cooperation is arrived at when δ is near 0.8; after that, its trend turns downward. Herein, it can be concluded that the parameter δ is really an obvious factor to influence the frequency of cooperation within the population, and when the cost-to-benefit ratio u is beyond a certain value, there exists the best value of δ to render the frequency of cooperation to achieve the peak.

Based on the above observations, it is necessary for us to further reveal the underlying reasons for the proposed mechanisms to promote the evolution of cooperation. On the one hand, according to previous works [29, 38, 41], heterogeneity within the population is an important factor to determine the evolutionary behavior of collective cooperation. Henceforth, dynamic adjustment of link weights between agents induced by agents' asymmetrical influence is the root cause of system heterogeneity. What is more, the larger the variance of the link weights among agents, the stronger the heterogeneity of the system. On the other hand, the role of connection types cannot be ignored, either. Thus, for different conditions, Fig. 6 not only presents the statistical results of link weight variance but also calculates the link weight distribution for different types. To be specific, the first line presents the results obtained at $u = 0.015$ while the last the row provides the results obtained at $u = 0.036$. In addition, panels (a) and (d) are the results of link wight variance; panels (b) and (e) are the results of link weight distribution for different types obtained at $\delta = 0.7$ while panels (c) and (f) are the same results obtained at $\delta = 0.9$. In Fig. 5, one has concluded that when u is quite small, the frequency of cooperation ρ_c continues to increase with the increase of δ ; while for quite larger u , ρ_c first undergoes increase and then decrease as δ grows. In panel (a) of Fig. 6, the link weight variance increases with the augmentation with δ , which seems to be in line with the conclusions of previous works [29, 38, 41]. However, the results in panel (d) are also similar to panel (a), which seems to contradict with the conclusions of previous works. Therefore, the pertinence between the occurrence of the evolution of cooperation and the heterogeneity does not apply to any scenarios, which elucidates that heterogeneity itself is not conducive to the evolution of cooperation. In other words, heterogeneity is not a necessary and sufficient condition for promoting the collective cooperation, which is consistent with the conclusion of previous work [49].

Since heterogeneity is not the direct cause of the evolution of cooperation, we consider whether some critical information can be found in the types of connections. It should be pointed out that we restrict the link weights to the interval $[1 - \delta, 1 + \delta]$. There is an interesting

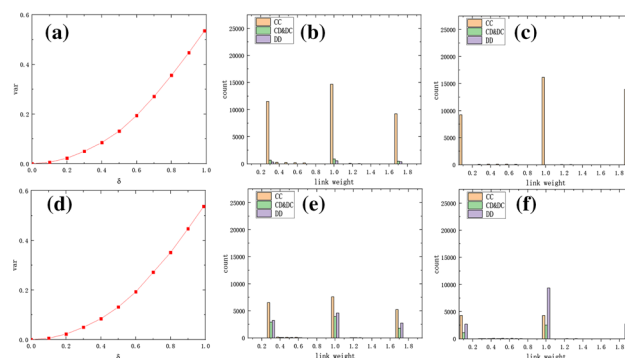


Fig. 6 Statistics of link weight variance and different types of link weight distribution under different conditions. The results of the first line are obtained at the cost-to-benefit ratio $u = 0.015$, and the ones of the second row are obtained at the cost-to-benefit ratio $u = 0.036$. Panels **a** and **d** are the results of statistics of link weight variance. Panels **b** and **e** are the results of different types of link weight distribution for $\delta = 0.7$ while panels **c** and **f** are the ones of link weight distribution obtained at $\delta = 0.9$. The simulations results are obtained at $MCS = 3 \times 10^4$, $L = 100$, $\Delta = 0.1$, $\beta = 1$ and $K = 0.1$

phenomenon in Fig. 6, that is, for the link weight distribution obtained under any conditions, expect that some of link weights are kept at the initial value of 1, and the rest of ones are almost distributed at the maximum or minimum regardless of the types of connections. By comparing the distribution results of the link weight obtained under different conditions, one can find that there are significant differences. For quite small value of u (e.g. $u = 0.015$), most of link weights occupy the $C - C$ connections and only small amount of link weights are distributed on other connections, which is the key factor for the cooperation to flourish, especially more link weights at the maximum. As $C - C$ connections enables the agents that interact with each other to gain stable returns, their relationships will become stronger and stronger. Moreover, when $\delta = 0.9$ the link weights at the maximum are much greater than those when $\delta = 0.7$, which explains the reason why the level of cooperation increases with the rise of δ when the cost-to-benefit ratio u is quite small. However, for quite larger value of u (e.g. $u = 0.036$), the situation has been drastically reversed. Whether $\delta = 0.7$ or $\delta = 0.9$, all three types of connections (i.e. $C - C$, $D - D$, and $C - D$ or $D - C$) emerge in large numbers. There is a clear difference in these two cases. For $\delta = 0.7$, the type of connection is dominated by $C - C$, while for $\delta = 0.9$, there are quite a large number of $D - D$ -type connection in the system. Moreover, $D - D$ -type connection in $\delta = 0.9$ is much more than those under case of $\delta = 0.7$. In particular, $D - D$ connections at the maximum value in $\delta = 0.9$ are much richer than the ones in $\delta = 0.7$. Furthermore, $C - D$ or $D - C$ connections can break down the tight cooperative clusters since cooperators in such a relationship have to endure exploitation from defectors, which is unfavorable in the evolution of cooperation. At this point, we have made clear the reason why

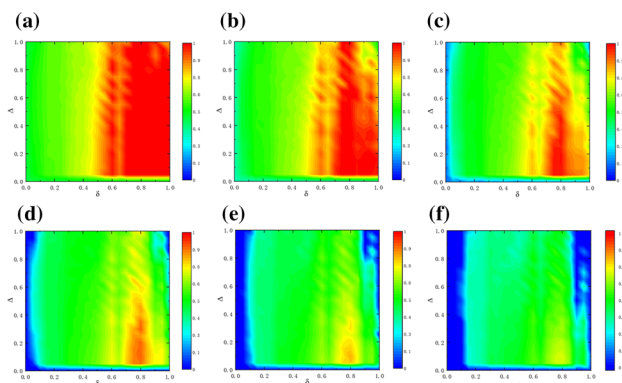


Fig. 7 Color phase encoding the frequency of cooperation ρ_c on $\delta - \Delta$ parameter plane for a series values of cost-to-benefit ratio u . Panels a–f are obtained at the cost-to-benefit ratio $u = 0.01, u = 0.015, u = 0.02, u = 0.025, u = 0.03, u = 0.035$, respectively. It can be found that when u is quite small, the level of cooperation increases with the augmentation of δ , while the parameter Δ seems to have no significant impact on the evolution of cooperation. Similar with previous discussion, when the cost-to-benefit ratio u exceeds to a certain value, the level of cooperation presents the first increase and then decrease with the increase δ . In addition, when the parameter δ reaches a certain value, the level of cooperation decreases as Δ gradually grows. All these observations suggest that there is an optimal combination $\delta - \Delta$ promoting the evolution of cooperation. All results are obtained at $L = 100, MCS = 3 \times 10^4, \beta = 1$ and $K = 0.1$

the level of cooperation goes through the first increase and the upcoming decrease with the increase of δ when the cost-to-benefit ratio u exceeds a certain threshold.

Finally, we need to have a comprehensive grasp of the proposed mechanism. Thus, Fig. 7 shows the color phase encoding the frequency of cooperation ρ_c within the $\delta - \Delta$ parameter plane for a series values of cost-to-benefit ratio u , in which the results from panels (a) to (f) are obtained at the values of $u = 0.01, u = 0.015, u = 0.02, u = 0.025, u = 0.03, u = 0.035$, respectively. Obviously, for different values of u , the trend of ρ_c changes with the parameter δ or Δ is quite diverse. To be specific, when u is fairly small (e.g. $u = 0.01$), the level of cooperation as a whole increases with the augmentation of δ , and the parameter Δ seems to have no significant impact on the level of collective cooperation. Moreover, for some particular combinations of parameters (δ, Δ) , cooperators can even dominate over the entire system. Nevertheless, with the increase of u , there are slight changes in these phases. For instance, when $u = 0.02$ or even larger, the level of cooperation first increases and then decreases with the increase of δ , and the peaks are almost at around $\delta = 0.8$, which is in line with the above-mentioned results. In addition, for some particular values of δ , the level of cooperation decreases with the increase of Δ . Combined with the these observations, we can conclude that there is an optimal combination of parameters (δ, Δ) that can best promote the evolution of cooperation.

4 Conclusions

To sum up, we propose a dynamic link weight adjustment game model with asymmetrical influence, in which each agent has been endowed with an influence attribute, and systematically explore the effect of dynamic adjustment link weight of influence induction on the evolution of cooperation. During the evolutionary process, if an agent’s strategy is learned by the focal player, it means that the agent’s influence can be expanded. Then, each agent will dynamically adjust the link weights between them by comparing the their influence. At last, link weights will be incorporated into the computational process of agents’ fitness, that is, link weights between agents can affect their fitness. It should be noted that although link weights are dynamically adjusted, this adjustment is only performed on a static network, that is, the connection between agents remains unchanged, which is different form dynamical network where the existing links can be rewired or the size of network can be grown [50–53].

After lots of simulations, it is confirmed that the currently proposed mechanism can tremendously foster the emergence of the collective cooperation within the spatial population playing the PDG. In addition, when the increment of agent’s influence $\beta \neq 0$, no mater how much the parameter β can be changed, the level of cooperation will not be significantly altered, which means that the parameter β is not the direct factor affecting the collective cooperation and the parameter β can only lead to the heterogeneity of individual influences. Moreover, when the normalized matrix payoff u is quite small, the level of cooperation increases as δ grows. Nevertheless, when the normalized payoff u exceeds a certain value, as δ increases, the frequency of cooperation ρ_c firstly increases and then declines, which indicates that there exists the best value of δ (around $\delta = 0.8$) that can lead to the highest level of cooperation. After analyzing the link weights under different conditions, we find that the heterogeneity facilitating the evolution of cooperation is not applicable to any scenario. In other words, the heterogeneity is not a necessary and sufficient condition for promoting the cooperation. Actually, the cooperation behaviors is often related to the type of links or connections. Since the $C - C$ pairwise interactions can allow agents to gain stable returns, while the $D - D$ ones can make agents get nothing. It is also important to note that $C - D$ or $D - C$ relationships render cooperators to endure the exploitation from defectors. Thus, cooperation can thrive when $C - C$ links dominate the system. Other types of relationships are unfavorable in the development of cooperation. In particular, $C - D$ or $D - C$ types of connections can even play a disruptive role in the evolution cooperation. In the end, by mapping $\delta - \Delta$ phase, we find an interesting phenomenon: When the matrix element u is quite small, the frequency of cooperation ρ_c increases as δ grows, while the increase of Δ and does not influence the level of cooperation at the stationary state. However, when the value of u

becomes very large, there is an optimal combination of parameters (δ, Δ) facilitating the evolution of cooperation, which means that too small or too large δ or Δ does not better favor the evolution of collective cooperation.

Considering the prevalence of link weight in nature and human society, we believe that our research can provide some valuable insights into the evolution of cooperation and offer some feasible advice for the study of this problem even if there are still some unrealistic assumptions in the proposed mechanism.

This project is partially supported by the Project of National Defense Science and Technology Innovation under Grant no. DF20190050.

Author contributions

CZ and XZ designed the model, analyzed the results and wrote the manuscript. All authors gave the final approval for publication.

Data Availability Statement This manuscript has no associated data or the data will not be deposited. [Authors' comment: There are no external data associated with the manuscript.]

References

1. T. Cluttonbrock, *Nature* **462**, 51 (2009)
2. C. Darwin, *Am. Anthropol.* **61**, 176 (1963)
3. G. Hardin, *Science* **162**, 1243 (1968)
4. J. Nash, *Proc. Natl. Acad. Sci. USA* **36**, 48 (1950)
5. M.A. Nowak, K. Sigmund, *Nature* **355**, 250 (1992)
6. T. Clutton-Brock, *Nature* **462**, 51 (2009)
7. R. Axelrod, W.D. Hamilton, *Science* **211**, 1390 (1981)
8. G.G. McNickle, R. Dybzinski, *Ecol. Lett.* **16**, 545 (2013)
9. G.M. Hodgson, K.N. Huang, *J. Evolut. Econ.* **22**, 345 (2012)
10. R. Kummerli, C. Colliard, N. Fiechter, B. Petitpierre, F. Russier, L. Keller, *Proc. R. Soc. B* **274**, 2965 (2007)
11. M. Perc, *New J. Phys.* **8**, 22 (2006)
12. F. Zhang, J. Wang, H.Y. Gao, X.P. Li, C.Y. Xia, *Eur. Phys. J. B* **94**, 22 (2021)
13. T. Lin, T. Alpcan, K. Hinton, *IEEE Syst. J.* **11**, 649 (2017)
14. X.Y. Li, T. Chen, Q. Chen, X.Y. Zhang, *Eur. Phys. J. B* **93**, 204 (2020)
15. J.M. Smith, G.R. Price, *Nature* **246**, 15 (1973)
16. M. Perc, O. Petek, S.M. Kamal, *Appl. Math. Comput.* **249**, 19 (2014)
17. S.S. Komorita, *J. Exp. Psychol.* **12**, 357 (1976)
18. M. Perc, A. Szolnoki, *Phys. Rev. E* **77**, 011904 (2008)
19. M. Perc, Z. Wang, *PLoS One* **5**, e15117 (2010)
20. A. Szolnoki, M. Perc, Z. Danku, *Phys. A* **387**, 2075 (2008)
21. Z. Wang, L. Wang, A. Szolnoki, *Eur. Phys. J. B* **88**, 124 (2015)
22. Q. Jian, X.P. Li, J. Wang, C.Y. Xia, *Appl. Math. Comput.* **396**, 125928 (2021)
23. M.A. Nowak, R.M. May, *Nature* **359**, 826 (1992)
24. X.H. Deng, Y. Liu, Z.G. Chen, *Physica A* **389**, 5173 (2010)
25. F.C. Santos, J.M. Pacheco, *Phys. Rev. Lett.* **95**, 098104 (2005)
26. X.K. Meng, S.W. Sun, X.X. Li, L. Wang, C.Y. Xia, J.Q. Sun, *Phys. A* **442**, 388 (2016)
27. J. Wang, W.W. Lu, L.N. Liu, L. Li, C.Y. Xia, *PLoS One* **11**, e0167083 (2016)
28. F. Fu, T. Wu, L. Wang, *Phys. Rev. E* **79**, 036101 (2009)
29. X.P. Li, S.W. Sun, C.Y. Xia, *Appl. Math. Comput.* **361**, 810 (2019)
30. Z.L. Xiao, X.J. Chen, *New J. Phys.* **22**, 023012 (2020)
31. W.J. Li, L.L. Jiang, M. Perc, *Appl. Math. Comput.* **391**, 125705 (2021)
32. A. Szolnoki, M. Perc, *New J. Phys.* **15**, 053010 (2013)
33. C.Y. Xia, X.P. Li, Z. Wang, M. Perc, *New J. Phys.* **20**, 75005 (2018)
34. W.X. Wang, J. Ren, G.R. Chen, B.H. Wang, *Phys. Rev. E* **74**, 056113 (2006)
35. W.W. Lu, J. Wang, C.Y. Xia, *Phys. Lett. A* **382**, 3058 (2018)
36. C.B. Sun, C. Luo, *Appl. Math. Comput.* **374**, 125063 (2020)
37. X.P. Li, H.B. Wang, G. Hao, C.Y. Xia, *Phys. Lett. A* **384**, 126414 (2020)
38. K.K. Huang, X.P. Zheng, Z.J. Li, Y.Q. Yang, *Sci. Rep.* **5**, 14783 (2015)
39. C. Shen, C. Chu, L. Shi, M. Perc, Z. Wang, *Roy. Soc. Open Sci.* **5**, 180199 (2018)
40. C. Chu, J.Z. Liu, C. Shen, J.H. Jin, Y.X. Tang, L. Shi, *Chaos Soliton Fractals* **104**, 28 (2017)
41. H. Guo, C. Chu, C. Shen, L. Shi, *Chaos Solitons Fractals* **109**, 265 (2018)
42. C. Hauert, G. Szabó, *Am. J. Phys.* **73**, 405 (2005)
43. Z. Wang, M. Perc, *Hashimoto Phys. Rev. E* **82**, 021115 (2010)
44. Q. Su, A. McAvoy, L. Wang, N.A. Nowak, *Hashimoto Proc. Natl Acad. Sci. USA* **116**, 25398 (2019)
45. G. Szabó, C. Tóke, *Phys. Rev. E* **652**, 69 (1998)
46. Y.T. Dong, G. Hao, J. Wang, C. Liu, C.Y. Xia, *Phys. Lett. A* **383**, 1157 (2019)
47. X.P. Li, H.B. Wang, C.Y. Xia, M. Perc, *Front. Phys-Lausanne* **7**, 125 (2019)
48. T. Wu, F. Fu, P.X. Dou, L. Wang, *Phys. A* **413**, 86 (2014)
49. M. Cardinot, J. Griffith, C. O'Riordan, *Phys. A* **493**, 116 (2018)
50. A. Szolnoki, M. Perc, *Eur. Phys. J. B* **67**, 337 (2009)
51. J.Q. Li, J.W. Dang, J.L. Zhang, *Appl. Math. Comput.* **369**, 124837 (2020)
52. T. Khoo, F. Fu, S. Pauls, *Sci. Rep.* **6**, 36293 (2016)
53. D.G. Rand, N.A. Christakis, *Proc. Natl. Acad. Sci. USA* **108**, 19193 (2011)